Optical polarization of excitons and trions under continuous and pulsed excitation in single layers of WSe_2

A.T. Hanbicki[a], M. Currie[b], G. Kioseoglou[c,d], C.S. Hellberg[a], A.L. Friedman[a], and B.T. Jonker[a]

[a] *Materials Science & Technology Division*, *Naval Research Laboratory*, Washington, DC 20375

[b] *Optical Sciences Division, Naval Research Laboratory*, Washington, DC 20375

[c] *Dept. of Materials Science and Technology, Univ. of Crete, Heraklion Crete, 71003, Greece*

[d] *Institute of Electronic Structure and Laser (IESL), Foundation for Research and Technology Hellas (FORTH), Heraklion Crete, 71110, Greece*

SUPPLEMENTARY INFORMATION

Section 1: **Raman of WSe_2**

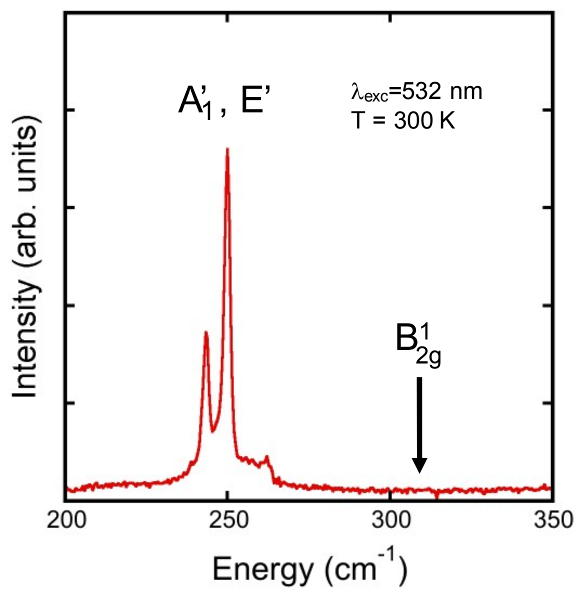

Fig. S1 – Raman spectrum of WSe_2 taken at room temperature with an excitation of 532 nm. The splitting of the A'_1 and E' peak near 252 cm^{-1} is consistent with a small amount of uniaxial strain in the system.[1] For multilayer material, a B^1_{2g} peak is expected at 309 cm^{-1}, therefore an absence of this peak is consistent with single layer material.[2]

Section 2: **Differential Reflectivity/Absorption**

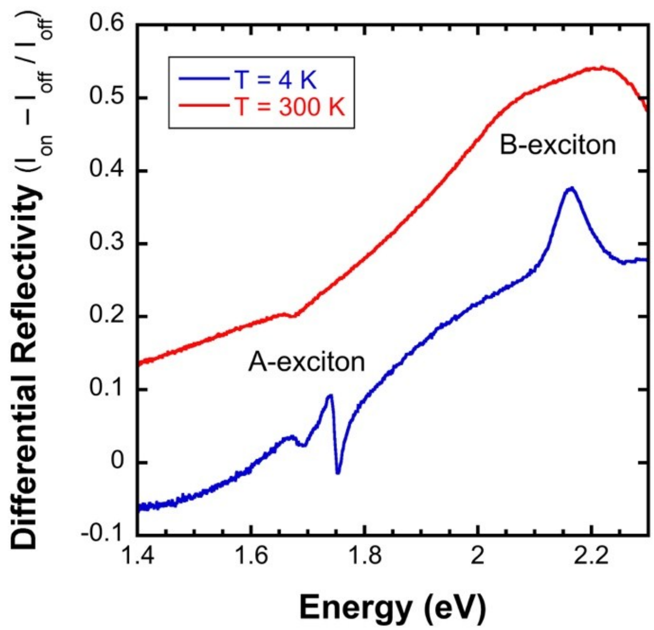

Fig. S2 – Differential reflectivity taken at 4 K and room temperature. The differential reflectivity is defined as the difference between the reflectivity measured with a white light source on the sample and the reflectivity measured just off the sample normalized to the reflectivity off the sample. Differential reflectivity is proportional to absorption and the A-exciton and B-exciton absorption features can be clearly seen in these spectra. For the A-exciton, both the neutral and charged exciton can be resolved at 4 K.

Section 3: **Power Dependence**

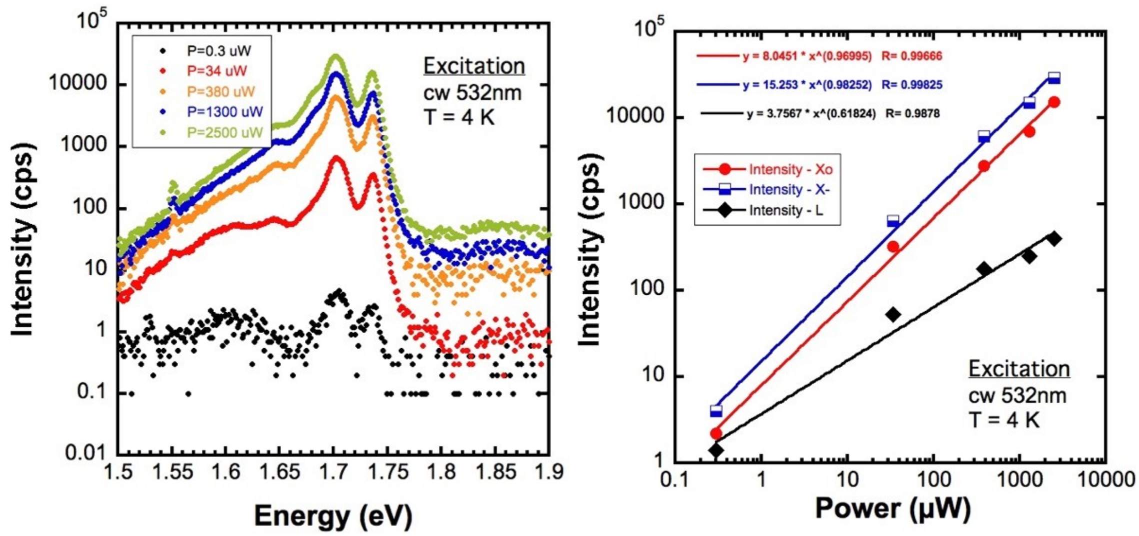

Fig. S3 – PL spectra of WSe_2 collected with cw excitation at 4 K for various powers. The left panel shows the raw spectra and the right panel is a summary of the various peak intensities as a function of power. Note that we are in the linear regime for all cw excitation.

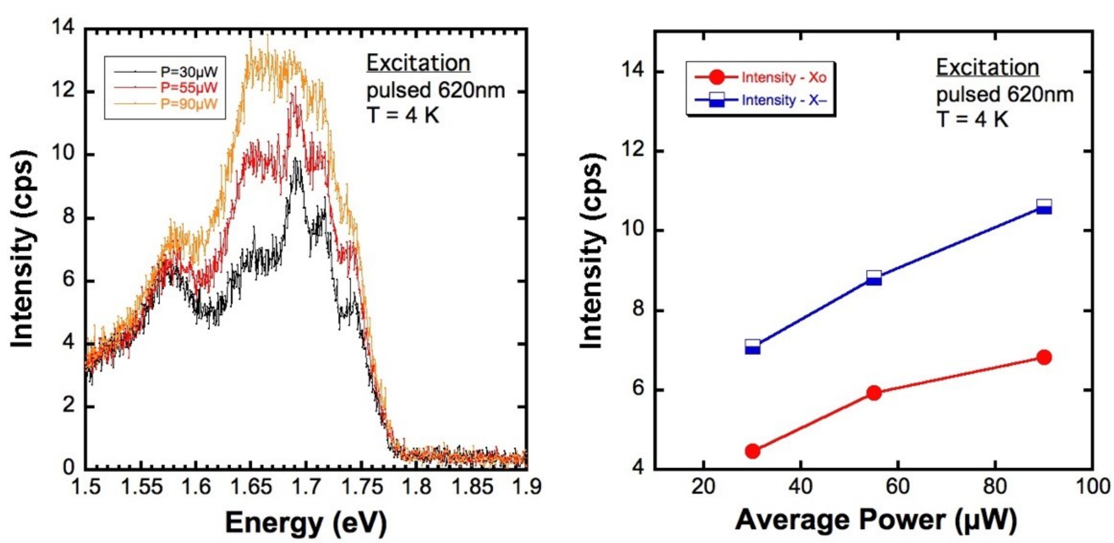

Fig. S4 – PL spectra of WSe_2 collected with pulsed excitation at 4 K for various powers. The left panel shows the raw spectra and the right panel is a summary of the various peak intensities as a function of power. Note the limited range of powers where reproducible PL is accessible using a pulsed laser. Below an average power of 30 μW, the PL intensity is difficult to observe, above about 90 μW the spectra begin to become permanently affected by the pulse.

Section 4: **Alternate fitting schemes**

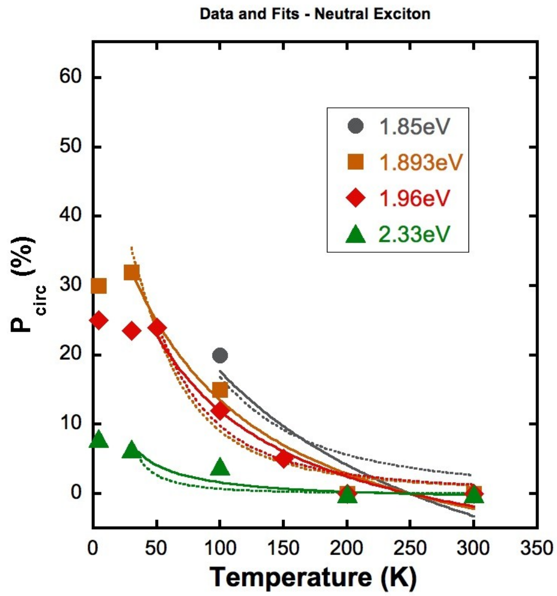

Fig. S5 – Temperature dependence of the circular polarization of the neutral exciton, X^0. The symbols are the data and the lines are fits. The solid line is a fit the model described in the main text where collisional broadening was considered and the dashed line is a fit where simple thermal broadening was used.[3]

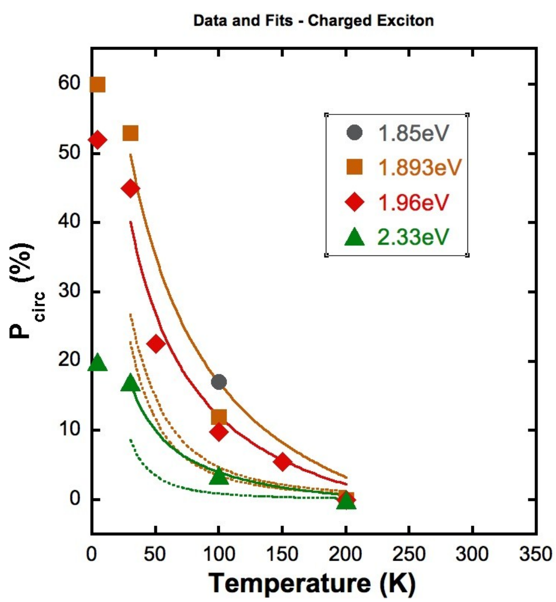

Fig. S6 – Temperature dependence of the circular polarization of the charged exciton, X^T. The symbols are the data and the lines are fits. The solid line is a fit the model described in the main text where collisional broadening was considered and the dashed line is a fit where simple thermal broadening was used.[3]

Section 5: **Raw helicity analyzed PL spectra and fits**

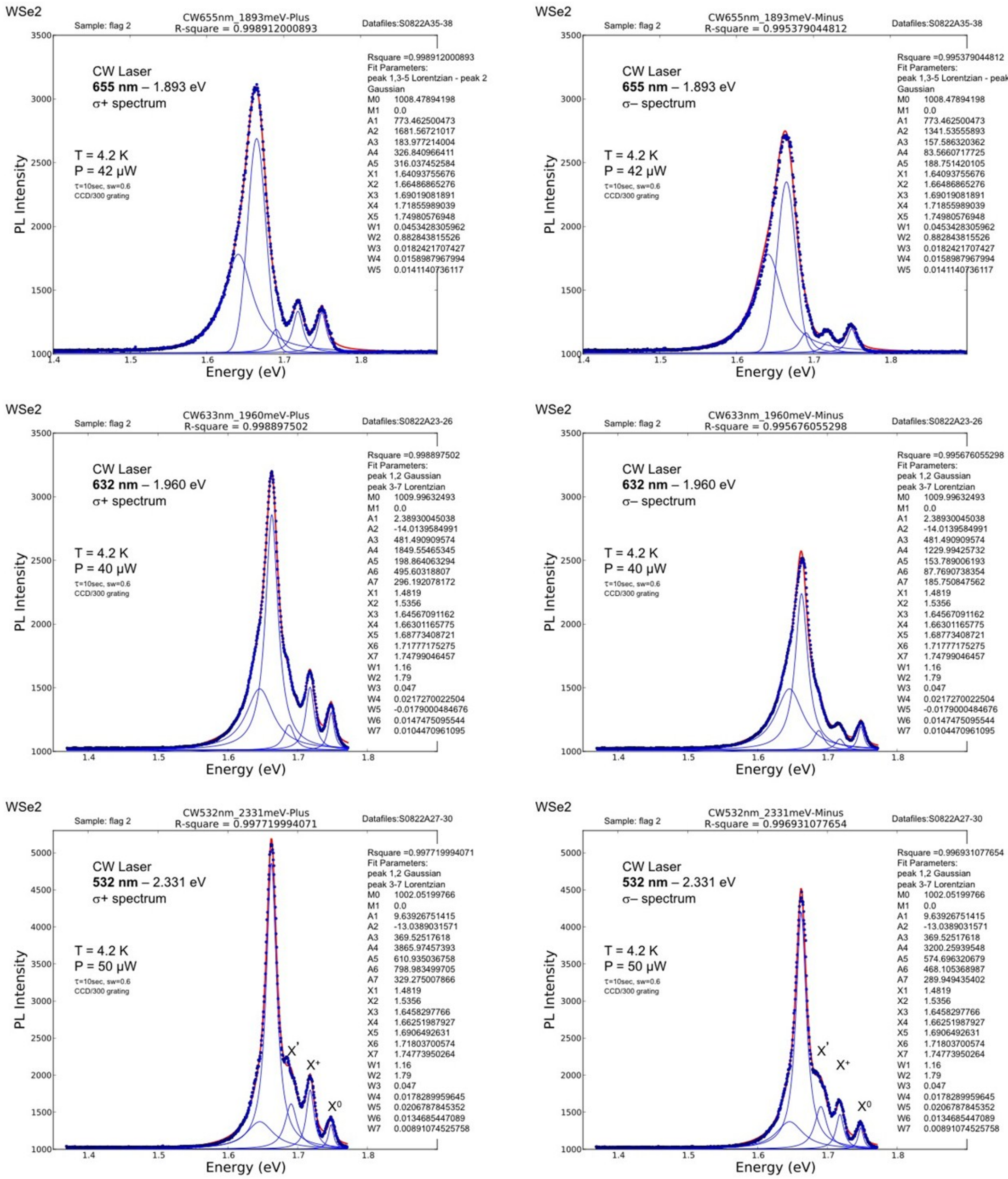

Fig. S7 – Raw data and fits of PL spectra taken with cw excitation at low temperature. Spectra on the left are analyzed for σ+ and spectra on the right are σ–. All peaks are fit in the σ+ spectra and then only the intensity is allowed to vary for the corresponding σ– spectra.

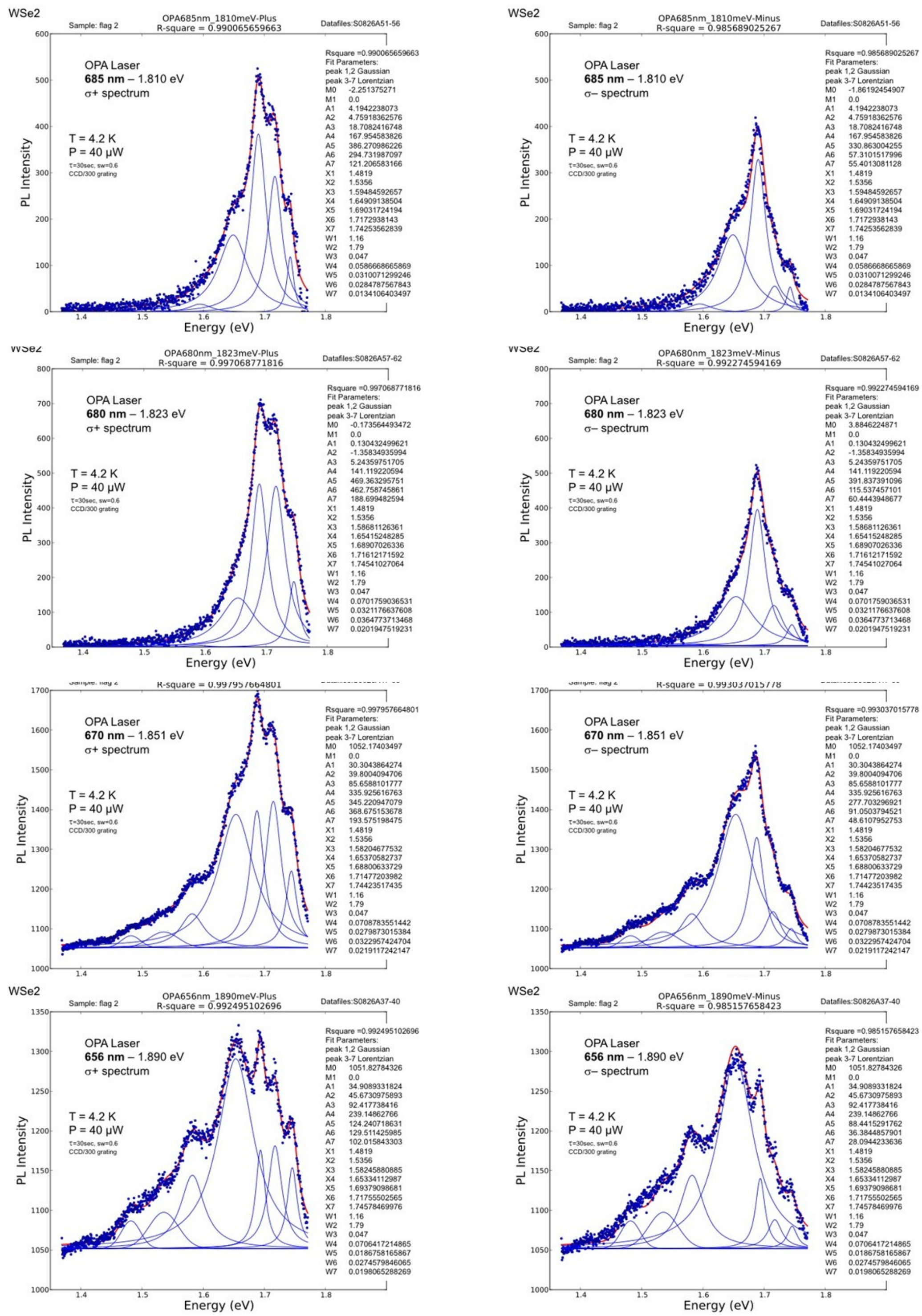

Fig. S8 – Raw data and fits of PL spectra taken with pulsed excitation at low temperature. Spectra on the left are analyzed for σ+ and spectra on the right are σ–. All peaks are fit in the σ+ spectra and then only the intensity is allowed to vary for the corresponding σ– spectra.

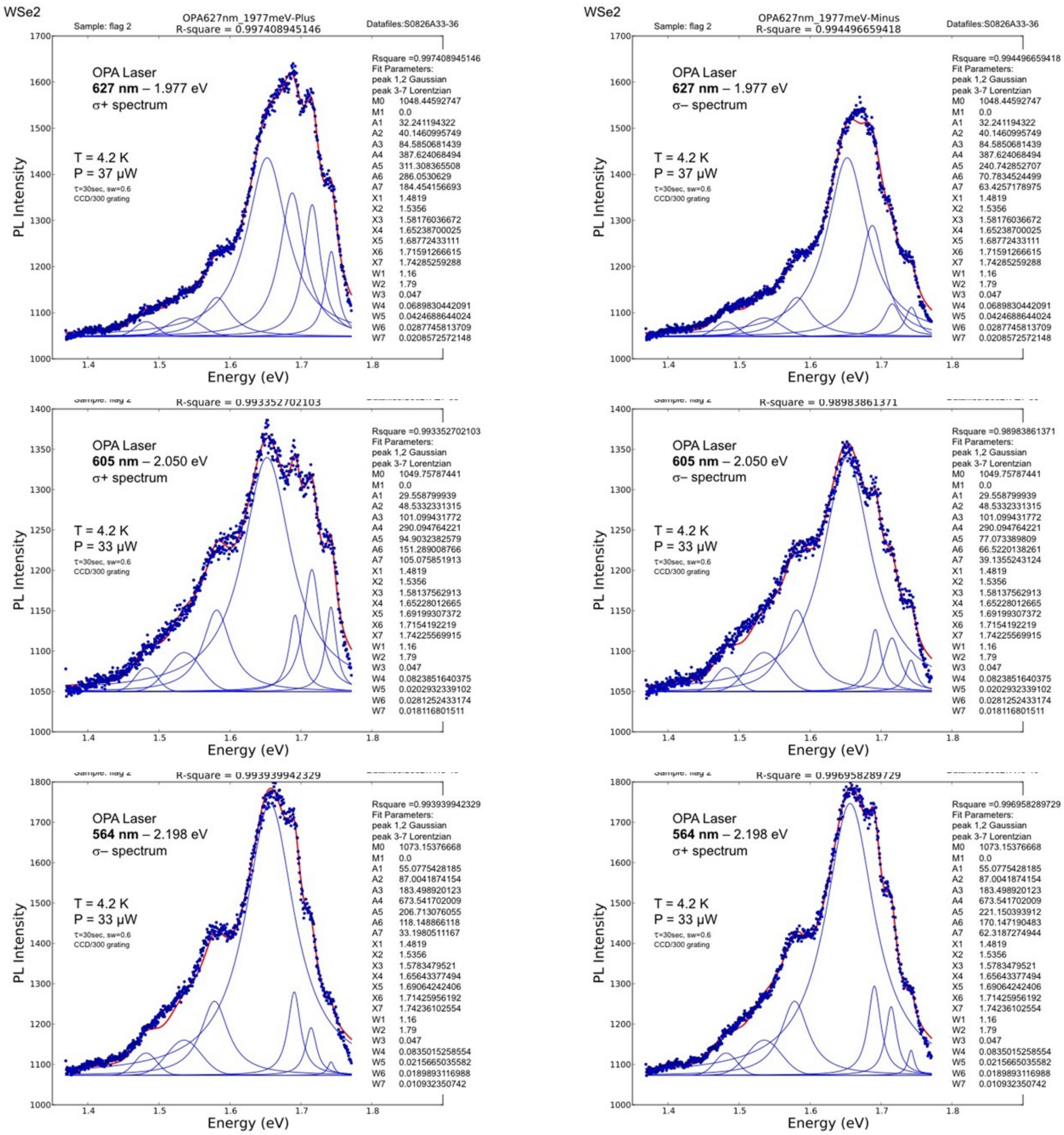

Fig. S9 – Raw data and fits of PL spectra taken with pulsed excitation at low temperature. Spectra on the left are analyzed for σ+ and spectra on the right are σ–. All peaks are fit in the σ+ spectra and then only the intensity is allowed to vary for the corresponding σ– spectra.

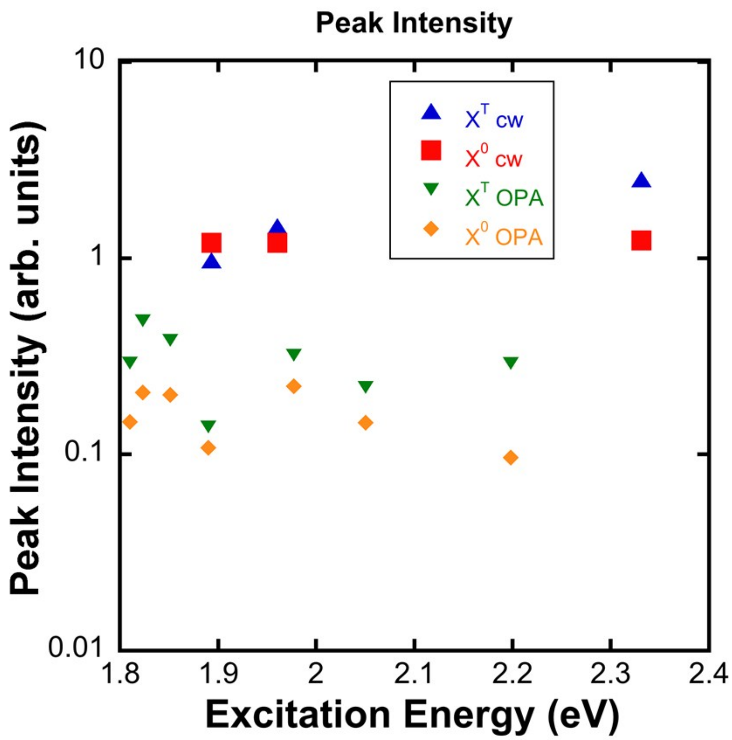

Fig. S10 – Summary of peak intensity vs. Excitation energy resolved for neutral excitons and trions using cw or pulsed excitation. Peak intensities are derived from the fits in figures S3-S6.

Section 6: **Table 1: WSe_2 parameters**

			A-exciton		
Reference	VB Splitting	CB Splitting	X^0	X^T	B-Exciton
This work	0.415 eV	—	1.745 eV	1.717 eV	2.16 eV
[4]-expmt	0.425 eV	—	1.75 eV	1.72 eV	2.17 eV
[5]-expmt	—	—	1.742 eV	1.713 eV	—
[6]-expmt	0.410 eV	—	1.751 eV	1.720 eV	2.16 eV
[7]-expmt	—	—	1.743 eV	1.708 eV	—
[8]-exp	0.480 eV	0.040 eV	1.73 eV	1.70 eV	2.21 eV
[9]-theory	0.466 eV	0.036 eV			
[10]-theory	0.490 eV	0.016 eV			

Section 7: **Rate equations and polarization**

To compute the polarization under pulsed excitation, we solve the following rate equations:

$$\frac{dN_K}{dt} = g - (\alpha + \beta + A)N_K + \beta N_{K'} \qquad \text{(S1)}$$

$$\frac{dN_{K'}}{dt} = g' - (\alpha + \beta + A)N_{K'} + \beta N_K \qquad \text{(S2)}$$

Here, N_K and $N_{K'}$ are the populations of excitons in the K and K' valleys, g and g' are the generation rates, α is the radiative recombination rate, A is the non-radiative recombination rate, and β is the spin/valley relaxation rate. We assume the pulse is much shorter than any other process and g=g'=0. The solution to these differential equations can be written as

$$N_K(t) = C_1(e^{-(\alpha + A)t} + e^{-(\alpha + A + 2\beta)t}) + C_2(e^{-(\alpha + A)t} - e^{-(\alpha + A + 2\beta)t}) \qquad \text{(S3)}$$

$$N_{K'}(t) = C_1(e^{-(\alpha + A)t} - e^{-(\alpha + A + 2\beta)t}) + C_2(e^{-(\alpha + A)t} + e^{-(\alpha + A + 2\beta)t}) \qquad \text{(S4)}$$

with constants C_1 and C_2.

At time zero,

$$N_K(t = 0) = 2C_1 \qquad \text{(S5)}$$

$$N_{K'}(t = 0) = 2C_2 \qquad \text{(S6)}$$

and the initial polarization is given by

$$P_0 = \frac{C_1 - C_2}{C_1 + C_2} \qquad \text{(S7)}$$

Assuming all excited carriers decay during the time between pulses, the emission intensities for each polarization are given by the following integrals:

$$I_+/\alpha = \int_0^\infty N_K(t)dt = \frac{C_1 + C_2}{\alpha + A} + \frac{C_1 - C_2}{\alpha + A + 2\beta} \qquad \text{(S8)}$$

$$I_{-}/\alpha = \int_0^\infty N_{K'}(t)dt = \frac{C_1 + C_2}{\alpha + A} + \frac{C_2 - C_1}{\alpha + A + 2\beta} \tag{S9}$$

Thus the observed polarization is

$$P_{circ} = \frac{I_{+} - I_{-}}{I_{+} + I_{-}} = \frac{\alpha + A}{\alpha + A + 2\beta}\frac{C_1 - C_2}{C_1 + C_2} = \frac{P_0}{1 + 2\beta/(\alpha + A)} \tag{S10}$$

REFERENCES:

1 H. Sahin, S. Tongay, S. Horzum, W. Fan, J. Zhou, J. Li, J. Wu and F. M. Peeters, *Phys. Rev. B*, 2013, **87**, 165409.

2 P. Tonndorf, R. Schmidt, P. Böttger, X. Zhang, J. Börner, A. Liebig, M. Albrecht, C. Kloc, O. Gordan, D. R. T. Zahn, S. M. de Vasconcellos and R. Bratschitsch, *Opt. Express*, 2013, **21**, 4908–4916.

3 S. Konabe, *Appl. Phys. Lett.*, 2016, **109**, 73104.

4 G. Wang, C. Robert, A. Suslu, B. Chen, S. Yang, S. Alamdari, I. C. Gerber, T. Amand, X. Marie, S. Tongay and B. Urbaszek, *Nat. Commun.*, 2015, **6**, 10110.

5 C. R. Zhu, K. Zhang, M. Glazov, B. Urbaszek, T. Amand, Z. W. Ji, B. L. Liu and X. Marie, *Phys. Rev. B*, 2014, **90**, 161302(R).

6 G. Wang, L. Bouet, D. Lagarde, M. Vidal, A. Balocchi, T. Amand, X. Marie and B. Urbaszek, *Phys. Rev. B*, 2014, **90**, 75413.

7 Y. You, X.-X. Zhang, T. C. Berkelbach, M. S. Hybertsen, D. R. Reichman and T. F. Heinz, *Nat. Phys.*, 2015, **11**, 477–481.

8 Z. Wang, L. Zhao, K. F. Mak and J. Shan, *Nano Lett.*, 2017, **17**, 740–746.

9 G.-B. Liu, W.-Y. Shan, Y. Yao, W. Yao and D. Xiao, *Phys. Rev. B*, 2013, **88**, 85433.

10 J. P. Echeverry, B. Urbaszek, T. Amand, X. Marie and I. C. Gerber, *Phys. Rev. B*, 2016, **93**, 121107.